J|A|C|S
ARTICLES

Published on Web 02/23/2010

Tunable High Performance Cross-Linked Alkaline Anion Exchange Membranes for Fuel Cell Applications

Nicholas J. Robertson, Henry A. Kostalik IV, Timothy J. Clark, Paul F. Mutolo,
Héctor D. Abruña, and Geoffrey W. Coates*

Department of Chemistry and Chemical Biology, Baker Laboratory, Cornell University,
Ithaca, New York 14853-1301

Received October 10, 2009; E-mail: coates@cornell.edu

Abstract: Fuel cells are energy conversion devices that show great potential in numerous applications ranging from automobiles to portable electronics. However, further development of fuel cell components is necessary for them to become commercially viable. One component critical to their performance is the polymer electrolyte membrane, which is an ion conductive medium separating the two electrodes. While proton conducting membranes are well established (e.g., Nafion), hydroxide conducting membranes (alkaline anion exchange membranes, AAEMs) have been relatively unexplored by comparison. Operating under alkaline conditions offers significant efficiency benefits, especially for the oxygen reduction reaction; therefore, effective AAEMs could significantly advance fuel cell technologies. Here we demonstrate the use of ring-opening metathesis polymerization to generate new cross-linked membrane materials exhibiting high hydroxide ion conductivity and good mechanical properties. Cross-linking allows for increased ion incorporation, which, in turn supports high conductivities. This facile synthetic approach enables the preparation of cross-linked materials with the potential to meet the demands of hydrogen-powered fuel cells as well as direct methanol fuel cells.

1. Introduction

Fuel cells are promising energy conversion devices for stationary and mobile applications; however, improving their performance and enhancing durability remain significant challenges.[1−3] Increasing the ionic conductivity and mechanical stability of solid polymer electrolyte membranes to achieve higher operating efficiencies are currently areas of intense research. Many low temperature (<100 °C) fuel cells employ a proton-exchange membrane (PEM) as the electrolyte. Of these, the most common is Nafion, which is a perfluorinated polymer containing pendant sulfonic acid side groups.[2,4] Nafion has good mechanical properties, excellent chemical stability, and exhibits high proton conductivities (~80 mS/cm at 25 °C) when properly hydrated.[5−8] However, Nafion's use is limited to acidic conditions and requires substantial dilution of carbon-based fuels (e.g., methanol) along with thicker membranes (less efficient) to prevent uncontrollable membrane swelling and fuel crossover.[3] Crossover occurs when fuel permeates the membrane from the anode to the cathode causing substantial performance losses.

A significant advantage of alkaline fuel cells (AFCs) over their acidic counterparts is greatly improved oxygen reduction kinetics as well as better fuel oxidation kinetics.[9−12] These improvements can lead to higher efficiencies and enable the use of nonprecious metal catalysts, greatly reducing the cost of the device. Indeed, hydrogen fueled AFCs can outperform all known low temperature fuel cells.[10] However, AFCs have traditionally employed liquid alkaline electrolytes containing metal hydroxides (e.g., potassium hydroxide) that react with CO_2 (present in the oxidant stream or fuel oxidation product when using carbon-based fuels) to form metal bicarbonates and subsequently carbonate salts. If sufficiently high levels of these salts are formed, they can precipitate out of solution, decreasing electrolyte conductivity and eventually obstructing electrode pores, both of which compromise power output.[13,14] Polymers with anchored organic cations hold great promise as alkaline anion exchange membranes (AAEMs) because their cations cannot aggregate with anions to form a crystal lattice. This approach therefore enables operation under alkaline conditions in the presence of CO_2.[10,15] Additionally, the direction of

---

(1) Borup, R.; et al. *Chem. Rev.* **2007**, *107*, 3904–3951.
(2) Diat, O.; Gebel, G. *Nat. Mater.* **2008**, *7*, 13–14.
(3) Hickner, M. A.; Ghassemi, H.; Kim, Y. S.; Einsla, B. R.; McGrath, J. E. *Chem. Rev.* **2004**, *104*, 4587–4611.
(4) Curtin, D. E.; Lousenberg, R. D.; Henry, T. J.; Tangeman, P. C.; Tisack, M. E. *J. Power Sources* **2004**, *131*, 41–48.
(5) Fontanella, J. J.; McLin, M. G.; Wintersgill, M. C.; Calame, J. P.; Greenbaum, S. G. *Solid State Ionics* **1993**, *66*, 1–4.
(6) Lee, C. H.; Park, H. B.; Lee, Y. M.; Lee, R. D. *Ind. Eng. Chem. Res.* **2005**, *44*, 7617–7626.
(7) Silva, R. F.; De Francesco, A.; Pozio, A. *J. Power Sources* **2004**, *134*, 18–26.
(8) Filipi, A.; B, M.; Gasteiger, H. A. *Electrochem. Soc. Trans.* **2008**, *16*, 1835–1845.
(9) McLean, G. F.; Niet, T.; Prince-Richard, S.; Djilali, N. *Int. J. Hydrogen Energy* **2002**, *27*, 507–526.
(10) Varcoe, J. R.; Slade, R. C. T. *Fuel Cells* **2005**, *5*, 187–200.
(11) Shen, P. K.; Xu, C.; Meng, H.; Zeng, R. *Adv. Fuel Cells* **2005**, 149–179.
(12) Spendelow, J. S.; Wieckowski, A. *Phys. Chem. Chem. Phys.* **2007**, *9*, 2654–2675.
(13) Cifrain, M.; Kordesch, K. V. *J. Power Sources* **2004**, *127*, 234–242.
(14) Gulzow, E.; Schulze, M. *J. Power Sources* **2004**, *127*, 243–251.
(15) Varcoe, J. R.; Slade, R. C. T.; Lam How Yee, E. *Chem. Commun.* **2006**, 1428–1429.

10.1021/ja908638d

hydroxide ion conduction opposes that of methanol crossover, thereby mitigating or possibly eliminating this process.[10,16]

PEM-based fuel cells have benefited from a large number of studies,[1,3] while AAEM technologies remain in their infancy. Nonetheless, Varcoe and Slade and co-workers have made great strides in this area by developing an AAEM containing polymeric benzyltrimethylammonium hydroxide ions anchored within a partially fluorinated, commercially available thin film.[17−21] Their system exhibits good conductivities (34 mS/cm at 50 °C), displays excellent performance under operating conditions, and is highly tolerant to CO_2.[22] Another noteworthy AAEM system is derived from films of chloromethylated polysulfones.[23−25] The resulting AAEMs display good conductivities (35 mS/cm at 30 °C) and highlight the importance of having continuous ionic domains throughout the material to provide pathways for ion conduction.[23] This requirement is supported by a recent study by Schmidt-Rohr and Chen of the relationship between the conductivity and morphology of Nafion.[26] Their findings suggest that microphase separation leads to hydrophobic regions that provide mechanical support for the material and hydrophilic regions with ionic nanochannels that provide a pathway for proton conduction. Cornelius and co-workers have recently reported a novel AAEM that employs a poly(phenylene) backbone, which exhibits good mechanical properties and excellent conductivity (50 mS/cm at 30 °C).[27] More recently, Zhang and co-workers disclosed an AAEM using a partially fluorinated polysulfone system that shows remarkable conductivities in excess of 60 mS/cm at 20 °C.[28] A variety of additional AAEMs based upon pre-existing polymer systems have also been described in recent literature, displaying a wide range of conductivities.[29−33] Additionally, there are hydrocarbon- and fluorocarbon-based commercially available AAEMs that yield impressive performances.[34,35] While all of these systems demonstrate great promise for AAEM science and establish the feasibility for alkaline membrane electrode assemblies, conductivity improvements are still necessary to reach performances comparable to present PEM technologies.

We have been developing new synthetic approaches to AAEMs in which the entire material contains tetraalkylammonium functionalities leading to continuous ionic domains, thereby allowing unobstructed ion conduction without the need for microphase separation. Materials with such high ionic content would generally suffer from significant swelling unless cross-links between polymer chains are installed to minimize this undesirable effect. DeSimone and co-workers recently used cross-linking to prepare a PEM system that exhibits conductivities that greatly surpass those of Nafion.[36] This approach enabled high ion content by mitigating swelling while providing mechanical integrity and led to extraordinarily high proton conductivities (254 mS/cm at ambient temperature). Additionally, we sought to develop a system that does not require postpolymerization modifications to attach tetraalkylammonium functionalities because cross-linking can hinder such reactions. Introduction of tetraalkylammonium groups to the monomer prior to the polymerization process would provide a more straightforward AAEM synthesis. We recently reported the use of the Grubbs second generation catalyst to copolymerize a tetralkylammonium-functionalized norbornene with dicyclopentadiene.[37] This system provided facile synthetic access to thin films under mild conditions, exhibited great material properties, and led to effective AAEMs by hydroxide ion-exchange following polymerization. Unfortunately, we were unable to surpass hydroxide conductivities of 30 mS/cm. We therefore turned our attention to developing a new system that would support higher ion conductivity while retaining good material properties and straightforward AAEM syntheses.

2. Results and Discussion

In an effort to improve conductivity, we prepared a variety of tetraalkylammonium-functionalized cross-linkers (two ammonium units and two olefins within the same molecule), such as compound **1** (Figure 1a), to enable cross-linking without the need for dicyclopentadiene; the use of the latter detracts from the ionic concentration and therefore the conductivity of the material. Compound **1** is readily synthesized in good yields from inexpensive starting materials, is readily scalable, and the dication salt is easily separated from organic impurities. Furthermore, polymerization using the air-stable Grubbs second generation catalyst eliminates the need for air- and moisture-free conditions during film casting, greatly simplifying membrane preparation. We polymerized **1** during a slow evaporation process, which led to uniform translucent thin films in near quantitative yields. Upon conversion to the hydroxide form, these materials became weak and difficult to handle. However, unlike materials developed from non-cross-linkable ammonium-functionalized cyclooctene monomers (analogous to **1** without the benzyl cross-linker), these materials would swell in water rather than dissolving, suggesting that cross-linking occurred upon polymerization of **1**. This behavior is similar to what we observed with our previous norbornene-based system.[37]

We found that addition of cyclooctene (COE) as a comonomer greatly improved the mechanical properties of the thin films.

---

(16) Dillon, R.; Srinivasan, S.; Arico, A. S.; Antonucci, V. *J. Power Sources* **2004**, *127*, 112–126.
(17) Slade, R. C. T.; Varcoe, J. R. *Solid State Ionics* **2005**, *176*, 585–597.
(18) Varcoe, J. R. *Phys. Chem. Chem. Phys.* **2007**, *9*, 1479–1486.
(19) Varcoe, J. R.; Slade, R. C. T. *Electrochem. Commun.* **2006**, *8*, 839–843.
(20) Varcoe, J. R.; Slade, R. C. T.; Yee, E. L. H.; Poynton, S. D.; Driscoll, D. J. *J. Power Sources* **2007**, *173*, 194–199.
(21) Varcoe, J. R.; Slade, R. C. T.; Yee, E. L. H.; Poynton, S. D.; Driscoll, D. J.; Apperley, D. C. *Chem. Mater.* **2007**, *19*, 2686–2693.
(22) Adams, L. A.; Poynton, S. D.; Tamain, C.; Slade, R. C. T.; Varcoe, J. R. *ChemSusChem* **2008**, *1*, 79–81.
(23) Hibbs, M. R.; Hickner, M. A.; Alam, T. M.; McIntyre, S. K.; Fujimoto, C. H.; Cornelius, C. J. *Chem. Mater.* **2008**, *20*, 2566–2573.
(24) Wang, G. G.; Weng, Y. M.; Chu, D.; Chen, R. R.; Xie, D. *J. Membr. Sci.* **2009**, *332*, 63–68.
(25) Zhou, J.; Murat, U.; Vega, J. A.; Kohl, P. A. *J. Power Sources* **2009**, *190*, 285–292.
(26) Schmidt-Rohr, K.; Chen, Q. *Nat. Mater.* **2008**, *7*, 75–83.
(27) Hibbs, M. R.; Fujimoto, C. H.; Cornelius, C. J. *Macromolecules* **2009**, *42*, 8316–8321.
(28) Wang, J. H.; Zhao, Z.; Gong, F. X.; Li, S. H.; Zhang, S. B. *Macromolecules* **2009**, *42*, 8711–8717.
(29) Xiong, Y.; Fang, J.; Zeng, Q. H.; Liu, Q. L. *J. Membr. Sci.* **2008**, *311*, 319–325.
(30) Park, J. S.; Park, S. H.; Yim, S. D.; Yoon, Y. G.; Lee, W. Y.; Kim, C. S. *J. Power Sources* **2008**, *178*, 620–626.
(31) Sollogoub, C.; Guinault, A.; Bonnebat, C.; Bennijima, M.; Akrour, L.; Fauvarque, J. F.; Ogier, L. *J. Membr. Sci.* **2009**, *335*, 37–42.
(32) Wu, L.; Xu, T. W. *J. Membr. Sci.* **2008**, *322*, 286–292.
(33) Wu, L.; Xu, T. W.; Wu, D.; Zheng, X. *J. Membr. Sci.* **2008**, *310*, 577–585.
(34) Moussaoui, R. E.; Martin, M. R. (Solvay, Societe Anonyme) US Patent Appl. 0124604, 2008.
(35) Yanagi, H.; Fukuta, K. *Electrochem. Soc. Trans.* **2008**, *16*, 257–262.
(36) Zhou, Z. L.; Dominey, R. N.; Rolland, J. P.; Maynor, B. W.; Pandya, A. A.; DeSimone, J. M. *J. Am. Chem. Soc.* **2006**, *128*, 12963–12972.
(37) Clark, T. J.; Robertson, N. J.; Kostalik, H. A., IV; Lobkovsky, E. B.; Mutolo, P. F.; Abruna, H. D.; Coates, G. W. *J. Am. Chem. Soc.* **2009**, *131*, 12888–12889.

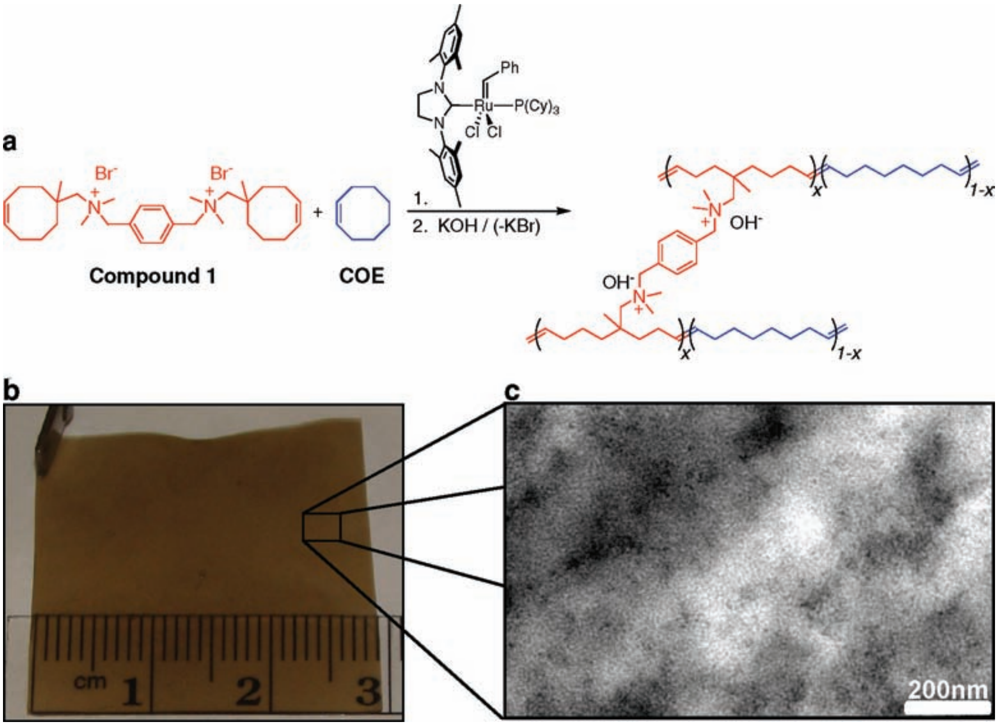

Figure 1. Monomer structure and film synthesis. (a) General AAEM synthesis includes combining **1** and COE in a chloroform/methanol cosolvent. Addition of the Grubbs second generation catalyst, followed by transfer to a metal dish at 35 °C and subsequent hydroxide ion exchange furnishes the desired AAEM. (b) Photograph of film in the bromide form placed on top of a ruler to demonstrate the clarity of films. (c) TEM of film in the bromide form showing a featureless, amorphous morphology.

Subsequent conversion of the films from the bromide form to the hydroxide form led to no discoloration, furnishing the final AAEM as a translucent pale brown thin film (Figure 1b). Figure 1c is a transmission electron micrograph of the amorphous material in the bromide form, which shows only random aggregations and no signs of well ordered structure, implying that these materials contain a relatively uniform distribution of tetraalkylammonium cations. Furthermore, differential scanning calorimetry analysis of the thin films in the bromide form revealed no melting temperature, whereas polycyclooctene produced using the Grubbs second generation catalyst showed a melting temperature of 37 °C. This supports the random incorporation of **1** and COE into the cross-linked polymer architecture. In an effort to maximize performance and gain a better understanding for this system, we prepared a variety of copolymers and studied their resulting mechanical properties and conductivites.

The relationship between the ratio of COE to **1** and hydroxide conductivity at room temperature is shown in Figure 2. The trend displays a maximum conductivity of 69 mS/cm with a composition of 1.5:1 mol equiv of COE to **1**. Higher loadings of **1** yielded materials with insufficient mechanical integrity for reliable measurements when pressed into the conductivity clamp. Diminished conductivity at higher COE loadings was expected because the ion concentration within the polymer membrane is decreased. The correlation between tensile strength and COE loading is also shown in Figure 2. Mechanical properties began to degrade as the composition moved below 2 equiv of COE and rapidly dropped off below 1.5 equiv. Increasing beyond 2 equiv of COE to **1** decreased the tensile strength, presumably because the cross-link density decreased as well. The overall trend between the two relationships shown in Figure 2 is noteworthy because it implies that there is a significant correlation between mechanical properties and conductivity.

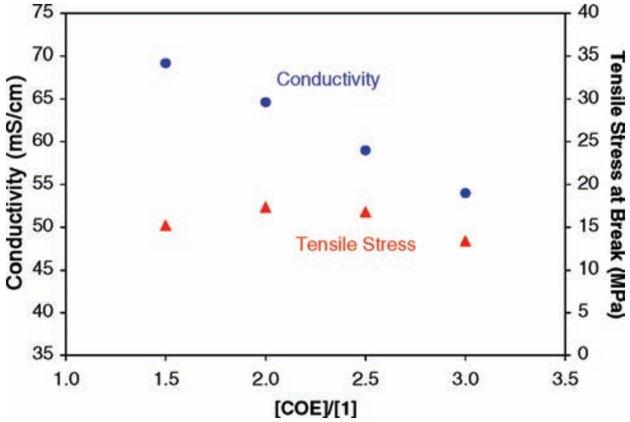

Figure 2. Influence of COE loading on conductivity and material properties at 22 °C. Conductivity values (●) were obtained from measurements of two separate films of the same composition and averaged. All films had a [**1**]:[catalyst] loading of 25:1. Tensile stress values (▲) are an average of multiple measurements with error bars omitted for clarity. All tensile stress errors are ±4.2 MPa or less and calculated at the 95% confidence level. See electronic Supporting Information for further details.

This correlation was further supported when we investigated the impact of catalyst loading on conductivity and mechanical properties (Figure 3). Conductivity generally increased with decreased catalyst loading. However, when the monomer to catalyst ratio was increased above 100:1 moles of olefin to moles of catalyst, the material became brittle and the conductivity rapidly decreased. This loss of mechanical properties and subsequent conductivity reduction is likely attributable to excessive swelling, which occurs when there is insufficient cross-link density to resist osmotic pressure.[38] Water uptake measurements act as a valuable aid in evaluating cross-link density. For the AAEMs with low catalyst loading, water uptake

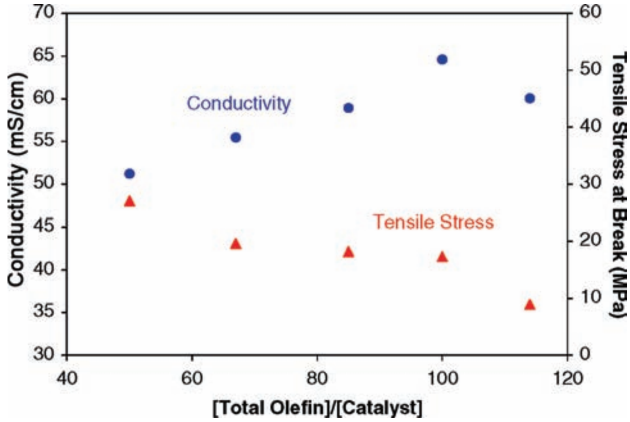

Figure 3. Influence of catalyst loading on conductivity and material properties at 22 °C. Conductivity values (●) were obtained from measurements of two separate films of the same composition and averaged. All films have a [COE]:[**1**] loading of 2:1. Tensile stress values (▲) are an average of multiple measurements with error bars omitted for clarity. All tensile stress errors are ±4.2 MPa or less and calculated at the 95% confidence level. See electronic Supporting Information for further details.

as high as 225% was observed, whereas increasing catalyst loading to increase cross-link density diminished water uptake nearly 2-fold. Increased cross-linking improves the mechanical strength of the membrane, but decreases the conductivity, which is a commonly observed trend.[29,39−41]

These materials are very promising candidates for fuel cell applications because they exhibit high hydroxide ion conductivity with impressive material properties. We postulate that these conductivities and mechanical properties are a direct result of cross-linking, enabling high ion content. A considerable benefit of this system is that it is highly tunable for the desired application. For example, films with lower cross-link density can be synthesized to maximize conductivity when a fuel such as hydrogen is used and swelling is less problematic. By contrast, COE loading can be varied to improve the material properties and higher cross-linking densities can be installed to combat swelling when carbon-based fuels are employed. Notably, there is no observable swelling of our AAEMs with high cross-link densities when immersed in 10 M aqueous methanol at 60 °C. All direct methanol fuel cells known to the authors, regardless of the concentration of methanol in the fuel reservoir, expose the electrolyte to only dilute aqueous methanol solutions of 1 molar concentration or lower, a value that is 1 order of magnitude below this system's tolerance. This is a very significant attribute for this system because using more concentrated fuels leads to higher energy densities.[3] Simply altering the quantities of reagents used controls the film thickness, and films can be reproducibly made as thin as 30 μm in the hydroxide form. While thinner films can be generated, self-adhesion becomes problematic when handling these materials.

Table 1. Conductivity Dependence upon Counterion[a]

counterion	conductivity (mS/cm) 22 °C	 50 °C
Br^-	1.8 ± 0.4	6.1 ± 0.5
Cl^-	10.0 ± 0.2	26.4 ± 0.6
HCO_3^-	8.9 ± 0.7	22 ± 1
CO_3^{2-}	14 ± 1	28 ± 1
OH^-	68.7 ± 0.8	111 ± 4

[a] All films had the composition of 1.5:1 [COE]:[**1**] with [total olefin]:[catalyst] loading of 90:1. Errors calculated at the 95% confidence level.

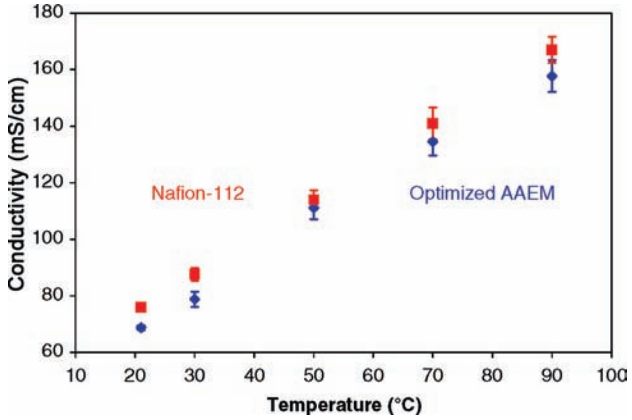

Figure 4. Impact of temperature on conductivity. Conductivities of Nafion-112 (■) and of the optimized AAEM (◆), which has a [COE]:[**1**] loading of 1.5:1 and [total olefin]:[catalyst] loading of 90:1 are shown. Errors are calculated at the 95% confidence level.

To further investigate the capability of this system, we prepared films with an optimized ratio of the comonomers ([COE]:[**1**] = 1.5:1) and catalyst loading ([total olefin]:[catalyst] = 90:1) to maximize conductivity of the polymer membrane. Table 1 shows the conductivities for the bromide, chloride, bicarbonate, carbonate, and hydroxide forms of this composition at room temperature and at 50 °C, demonstrating the excellent conductivity and scope of this system. We observed a hydroxide conductivity of 111 mS/cm at 50 °C. By comparison, Varcoe and Slade's AAEMs exhibited 34 mS/cm and 22 mS/cm at 50 °C for the hydroxide and carbonate forms, respectively.[21] Cornelius and co-workers observed conductivities of 50 mS/cm at 30 °C for their poly(phenylene)-based system in the hydroxide form,[27] and Zhang and co-workers' system showed 87 mS/cm at 60 °C.[28] Furthermore, if carbonate and bicarbonate species should form in the membrane under operating conditions, the conductivities of our system are still significant, suggesting that performance losses will not be detrimental to overall performance. Indeed, it has even been shown that power densities can be as good or better when CO_2 is introduced into an AFC due to improved electrode kinetics in the presence of carbonate.[22,42] The ion-exchange capacity of the material is 2.3 ± 0.2 mmol OH^-/g material which compares favorably to the theoretical value (2.8 mmol OH^-/g material), indicating that cross-linking enables high ion incorporation.

Figure 4 illustrates the correlation between conductivity and temperature for Nafion 112 (measured using our experimental set up, which correlates well with literature values)[5−8] and our AAEM with the composition optimized for conductivity. The conductivity of this material steadily increases with temperature and exhibits conductivities comparable to Nafion up to 90 °C when immersed in water. These hydroxide conductivities are

---

(38) Tsang, E. M. W.; Zhang, Z.; Shi, Z.; Soboleva, T.; Holdcroft, S. *J. Am. Chem. Soc.* **2007**, *129*, 15106–15107.
(39) Bauer, B.; Strathmann, H.; Effenberger, F. *Desalination* **1990**, *79*, 125–144.
(40) Jeong, M. H.; Lee, K. S.; Lee, J. S. *Macromolecules* **2009**, *42*, 1652–1658.
(41) Sata, T.; Teshima, K.; Yamaguchi, T. *J. Polym. Sci., Part A: Polym. Chem.* **1996**, *34*, 1475–1482.
(42) Unlu, M.; Zhou, J.; Kohl, P. A. *Electrochem. Solid-State Lett.* **2009**, *12*, B27–B30.

significantly higher than any reported AAEMs to date and demonstrate the potential of this system. When one considers that the mobility of protons is inherently faster than that of hydroxide ions in dilute solution by a factor of 1.77,[23] it is even more intriguing that our material conducts hydroxide ions nearly as well as Nafion conducts protons over this temperature range.

The long-term stability of AAEMs is generally of concern due to known degradation pathways for tetraalkylammonium ions under alkaline conditions (β-hydrogen elimination, direct nucleophilic substitution at an α-carbon, or nitrogen ylide formation).[10,43−45] We are confident that these materials will exhibit good durability because the tetraalkylammonium ions are devoid of β-hydrogens and are structurally analogous to existing systems that already demonstrate good stability under alkaline conditions.[21,39,46] Additionally, the high ion content of these materials makes them very hydrophilic, which will help retain water within the membrane to reduce the reactivity of the hydroxide ions, promote conductivity, and protect the ammonium ions.[43−45] More importantly, the high conductivity of this system will facilitate low temperature fuel cell operation, greatly diminishing degradation rates.

3. Conclusions

We have successfully developed a facile new route for AAEM synthesis that provides multiple points of variation to allow tuning of the system for the desired application. These AAEMs exhibit high hydroxide ion conductivity, while retaining good mechanical strength, making them very exciting candidates for fuel cell applications. We are beginning to study the performance and durability of these materials under operating conditions using in-house fuel cell test stations with methanol and hydrogen as fuels and are developing methods for hydrogenating the polymer backbone to improve long-term stability. Moreover, we are working to develop a soluble, non-cross-linked variant of this system, which will provide solvent processability and facilitate membrane preparation.

Acknowledgment. This material is based on work supported as part of the Energy Materials Center at Cornell, an Energy Frontier Research Center funded by the U.S. Department of Energy, Office of Science, Office of Basic Energy Sciences under Award Number DE-SC0001086, as well as a grant from the U.S. Department of Energy (DE-FG02-03ER46072). Additionally we thank Dr. Ivan Keresztes and Anthony Condo for assistance with ^{1}H and ^{13}C NMR and high resolution mass spectrometry, Dr. Jagdish Tewari for help with mechanical testing, and John Grazul for TEM analysis, as well as Drs. Lewis Fetters, Bryan Pivovar, and James Boncella for helpful discussions. T.J.C. is grateful to the NSERC of Canada for a Postdoctoral Fellowship.

Supporting Information Available: All experimental procedures and characterization of synthetic intermediates of **1**. Photograph of film synthesis assembly and TEM images as well as complete data sets for Figures 2 and 3 and a sample Nyquist plot. Complete authorship listing for ref 1. This information is available free of charge via the Internet at http://pubs.acs.org.

JA908638D

---

(43) Chempath, S.; Einsla, B. R.; Pratt, L. R.; Macomber, C. S.; Boncella, J. M.; Rau, J. A.; Pivovar, B. S. *J. Phys. Chem. C* **2008**, *112*, 3179–3182.

(44) Einsla, B. R.; Chempath, S.; Pratt, L. R.; Boncella, J. M.; Rau, J.; Macomber, C.; Pivovar, B. S. *Electrochem. Soc. Trans.* **2007**, *11*, 1173–1180.

(45) Macomber, C. S.; Boncella, J. M.; Pivovar, B. S.; Rau, J. A. *J. Therm. Anal. Calorim.* **2008**, *93*, 225–229.

(46) Sata, T.; Tsujimoto, M.; Yamaguchi, T.; Matsusaki, K. *J. Membr. Sci.* **1996**, *112*, 161–170.